

Highly Efficient Separation of Trivalent Minor Actinides by a Layered Metal Sulfide ($KInSn_2S_6$) from Acidic Radioactive Waste

Chengliang Xiao,^{†,‡,§,ID} Zohreh Hassanzadeh Fard,[‡] Debajit Sarma,[‡] Tze-Bin Song,[‡] Chao Xu,^{*,§,ID} and Mercouri G. Kanatzidis^{*,‡,§,ID}

[†]School for Radiological and Interdisciplinary Sciences (RAD-X) and Collaborative Innovation Center of Radiation Medicine of Jiangsu Higher Education Institutions, Soochow University, Suzhou 215123, China

[‡]Department of Chemistry, Northwestern University, 2145 Sheridan Road, Evanston, Illinois 60208, United States

[§]Collaborative Innovation Center of Advanced Nuclear Energy Technology, Institute of Nuclear and New Energy Technology, Tsinghua University, Beijing 100084, China

Supporting Information

ABSTRACT: The elimination of trivalent minor actinides (Am^{3+} , Cm^{3+}) is of great concern for the safe management and operation of nuclear waste geological repository and environmental remediation. However, because of the effects of protonation, most of the present sorbents exhibit inferior removal properties toward minor actinides at low pH values. Finding stable ion-exchangers with high sorption capacities, fast kinetics, and good removal toward minor actinides from highly acidic solution remains a great challenge. This work reports a new family member of KMS materials with a robust acid-stable layered metal sulfide structure ($KInSn_2S_6$, KMS-5) bearing strong affinity toward trivalent minor actinides. KMS-5 can simultaneously separate trivalent ^{241}Am and ^{152}Eu from acidic solutions below pH 2 with high efficiency (>98%). The ion-exchange kinetics is extremely fast (<10 min) and the largest distribution coefficient is as high as 5.91×10^4 mL/g. KMS-5 is also capable of efficiently removing ^{241}Am from acidic solution containing various competitive cations in large excess. In addition, the ion exchange process of ^{241}Am by KMS-5 is reversible and the loaded material can be easily eluted by high concentration of potassium chloride. This work represents the first case for efficient minor actinides removal from highly acidic solution using layered metal sulfide materials.

The environmental issues associated with the development of nuclear power are of great concern due to the high radiotoxicity of used fuels.¹ Minor actinides (Am, Cm) are the predominant remaining long-term, radiotoxic elements after recycling uranium and plutonium by the PUREX (plutonium and uranium extraction) process, which will pose potential long-term risk to the environment.² One optional strategy entitled partitioning and transmutation (P&T) seems promising to first separate minor actinides from high level liquid waste (HLLW) and then transmute them into stable or low radiotoxic radionuclides by accelerator driven subcritical system (ADS).³ It is beneficial for the management and operation of geological repositories because it minimizes the radiotoxicity, volume, and heat load of nuclear waste.

The separation of minor actinides is an essential step to allow transmutation. Most of the separation processes⁴ are developed on the basis of solvent extraction principle and have common disadvantages such as large amounts of (toxic, volatile) organic solvent usage, third phase formation, radiation decomposition of solvents, and large volumes of secondary radioactive waste. Solid extraction materials such as sorbents or ion exchangers can overcome these disadvantages,⁵ while holding the merits in separation minor actinides from HLLW. In addition, sorption or ion exchange methods can be efficient, simple, low-cost processes, particularly suitable for removing contaminated minor actinides at low levels and point-of-use applications.⁶

Sodium titanates⁷ and Zr/Sn phosphates/phosphonates⁸ as well as recently emerging inorganic sorbents such as carbon nanotubes,⁹ functional mesoporous silica,¹⁰ graphene oxide,¹¹ and porous aromatic framework (PAF)¹² have been reported to have high affinity toward americium. However, in highly acidic solutions (pH < 2), these sorbents exhibited very low uptake. For example, Long et al.¹² reported a carboxylic acid-functionalized PAF, BPP-7 (Berkeley Porous Polymer-7), for extraction of actinides from aqueous mixtures. This sorbent showed high sorption ability toward Am^{3+} with a distribution coefficient (K_d) of $\sim 5 \times 10^3$ mL/g at pH 2.5–4.0, whereas the K_d value falls to only 20 mL/g at pH 1.5. Graphene oxide can achieve nearly complete removal of Am^{3+} at pH 3–11, but the uptake deceases considerably at lower pH with only around 5% removal at pH 1.5.¹¹ One should bear in mind that most of the HLLW is highly acidic and the resulting polluted water by nuclear accidents will also be acidic. Thus, seeking stable materials with high sorption capacities, fast kinetics, and good selectivity toward trivalent minor actinides in highly acidic solution remains a great challenge.

Previously, we have confirmed that layered metal sulfides exhibited exceptional ion exchange properties toward Cs^+ , Sr^{2+} , UO_2^{2+} , rare earth elements, and heavy metals.¹³ However, similar to other sorbents, the low uptake at low pH is still a problem for these materials. For example, $K_{2-x}Mn_xSn_{3-x}S_6$ (KMS-1) achieves $\sim 100\%$ uranium removal at pH 3–9 in contrast to only $\sim 35\%$ capture at pH 2.^{13e} In this work, we

Received: September 30, 2017

Published: November 6, 2017



replace divalent Mn^{2+} (KMS-1)^{13a} and Mg^{2+} ions (KMS-2)^{13f} with trivalent In^{3+} to obtain a new family member of KMS materials, $KInSn_2S_6$ (KMS-5), for minor actinides capture from highly acidic solution. The introduction of indium with higher charge makes KMS-5 more stable toward acid and resistant to the competitive proton exchange. Even at pH 1, the removal of ^{241}Am still reaches as high as 97% with $K_d > 10^4$ mL/g. This work represents the first case for efficient trivalent minor actinides removal from highly acidic solution using layered metal sulfide materials.

The KMS-5 ion exchanger was prepared by a high temperature solid-state reaction at 800 °C with K_2CO_3 / K_2S_6 , In, Sn, and S as raw materials (see SI). The obtained KMS-5 is a golden yellow-like compound (Figure 1a,b) and SEM image

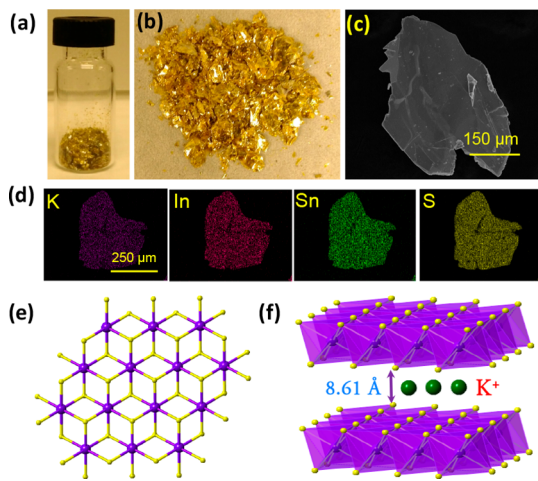


Figure 1. Morphology and structure of KMS-5. (a, b) Typical photos, (c) SEM image, (d) EDS mapping, (e) layered structure viewed down the *c*-axis, and (f) polyhedral representation of the typical layers along the *c*-axis. The purple, yellow, green colors denote Sn/In, S, and K, respectively.

shows it is flaky with a size of hundreds of micrometers (Figure 1c). EDS mapping (Figure 1d) and ICP-OES measurements confirm that KMS-5 is composed of K, In, Sn, and S elements and the formula is determined as $KInSn_2S_6$ (Figure S1). Single crystal diffraction shows that KMS-5 is a typical layered structure (Figure 1d,e) in the space group of $R\bar{3}m$ with a unit cell of $a = b = 3.6803(1)$ Å, $c = 26.1276(16)$ Å (Table S4). The layer is constructed by (In/Sn) S_6 octahedra with In and Sn atoms occupying in the same position. The disordered K^+ in the gallery to balance the charge can be facilely exchanged by other metal ions. The purity of KMS-5 phase was confirmed with powder X-ray diffraction (Figure S2).

To evaluate the capture ability of KMS-5 toward trivalent minor actinides and its potential for HLLW treatment and environmental remediation, ^{241}Am and ^{152}Eu ion-exchange kinetics, capacity, acid-stability as well as pH effect on the exchange properties were performed at room temperature. The concentrations of ^{241}Am and ^{152}Eu were measured by liquid scintillation counting (LSC).¹⁴ The ^{241}Am ion-exchange kinetics of KMS-5 was conducted with initial concentration of 4264 cpm/100 μ L ($\sim 5 \times 10^{-3}$ ppm) at a liquid-solid ratio (V/m) of 1000 mL/g and pH 2. As shown in Figure 2a, the concentration of ^{241}Am in the aqueous solution decreases rapidly as the contact proceeded. At initial 5 min, the concentration of ^{241}Am is reduced to 476 counts, correspond-

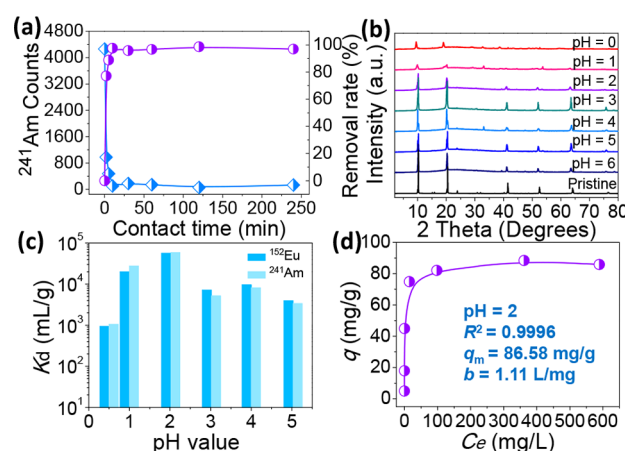


Figure 2. (a) Sorption kinetics of ^{241}Am by KMS-5 at pH 2. (b) Stability of KMS-5 after immersed in aqueous solution with different pH values (0–6) for 24 h as demonstrated by PXRD patterns. (c) Effect of pH (0.5–5) on the distribution coefficients of ^{241}Am and ^{152}Eu . (d) Sorption isotherm of Eu^{3+} by KMS-5 at pH 2 as a function of metal concentration (5–675 ppm).

ing to ~90% removal. After only 10 min, the ion-exchange process reaches an equilibrium with ~98% removal. These results show that KMS-5 can capture ^{241}Am from an acidic solution very fast. By contrast, the sorption of Am^{3+} onto BPP-7 does not reach equilibrium within 180 min.¹² The uptake of Am^{3+} by sodium titanate reaches steady-state only after 120 min.⁷ The ultrafast ion-exchange kinetics can significantly decrease the contact time between the sorbents and radioactive solution, lowering the damage induced by radiation and eliminating the releasing risk on an accidental emergency occasion.

To confirm the stability of KMS-5 in acidic solution, we immersed 10 mg of KMS-5 crystals in 10 mL of aqueous solution with different pH values in the range of 0–6 adjusted by HNO_3 for 24 h. As shown in Figure 2b, the PXRD patterns of immersed materials in the range of 2–6 are almost the same as the pristine KMS-5 crystals, which indicates that KMS-5 could hold its original crystal structure over this pH range. At pH 1, the proton starts to competitively exchange with K^+ and the KMS-5 materials are completely transformed into its corresponding H-type structure at pH 0 (Figures 2b, S3, and S4). SEM images (Figure S5) show that the interlayer became swollen. Despite this, the layered structure still survives even at pH = 0. In addition, the ICP measurements show that the maximum indium concentration in aqueous solution at pH = 2 was 2.11 ppm, corresponding to 1.07% of the mass dissolved from KMS-5 (Table S2), which also indicates that KMS-5 is very stable under our experimental conditions.

The effect of pH values varying from 0 to 5 on the removal of ^{241}Am and ^{152}Eu by KMS-5 was studied at a liquid/solid ratio of 1000 mL/g. In the entire pH range tested, all the K_d values of ^{241}Am and ^{152}Eu are above 10^3 mL/g (Figure 2c and Table S5). Particularly, the capability of KMS-5 to capture ^{241}Am and ^{152}Eu from strongly acidic solution is impressive. The K_d value of ^{241}Am at pH 2 is 5.91×10^4 mL/g (~98.3% removal) and it is 2.79×10^4 mL/g (~96.5% removal) at pH 1. Even at pH 0.5 (~ 0.32 mol/L HNO_3), it still has a removal percentage of ^{241}Am with 51.5% ($K_d \sim 1.06 \times 10^3$ mL/g). Such high K_d values reveals a remarkable attraction Am^{3+} and Eu^{3+} toward KMS-5. By comparison, the K_d values of Am^{3+} by monosodium

titanate,⁷ cerium vanadate,¹⁵ and functional mesoporous silica^{10b} are lower than 100 mL/g at pH 1 (Table S6). Though Zr/Sn(IV) phosphonates⁸ shows extremely high affinity toward Am^{3+} at pH 3, the K_d values are greatly decreased to $<10^3$ mL/g at pH 1. Due to competitive protonation, the uptakes of Am^{3+} onto BPP-7¹² and graphene oxide¹¹ are also extremely low under strongly acidic condition. In addition, the separation properties of ^{241}Am and ^{152}Eu by KMS-5 are almost the same, indicating that KMS-5 has no selectivity toward ^{241}Am even having soft sulfur donors. However, it still can be applied in the simultaneous separation of trivalent minor actinides and lanthanides from HLLW and the environmental remediation of trivalent actinide-contaminated acidic water.

Considering ^{241}Am and ^{152}Eu exhibit similar uptake behaviors by KMS-5, we use stable Eu^{3+} to simulate Am^{3+} for obtaining the ion-exchange capacity to avoid the use of large amounts of Am^{3+} with extremely high radioactivity. The ion-exchange capacity equilibrium as a function of Eu^{3+} concentration was performed at pH 2. The isotherms curve shown in Figure 2d is well fitted to the Langmuir model (Figure S6) rather than the Freundlich model (Figure S7). The maximum capacity is calculated to be ~ 87 mg Eu/g KMS-5 (Table S7), which is exactly consistent with the theoretical ion-exchange capacity (~ 86 mg/g). Because most sorbents exhibit low uptake at this low pH, few sorption capacities at pH 2 have been reported. In spite of this, the capacity of KMS-5 is still higher than the values (1.51–64.3 mg/g) of traditional sorbents (zeolite, activated carbon, and clay minerals)¹⁶ and comparable to the recently emerging sorbents (graphene oxide, nanocarbon, FJSM-SnS)¹⁷ performed at high pH (see Table S8). In addition, the Langmuir constant (b) related to the free energy of the sorption in this case is 1.11 L/mg, which is much higher than those of Cs^+ (0.07 L/mg)^{13b} and Sr^{2+} (0.44 mL/g)^{13a} sorbed on layered metal sulfides.

The Eu-exchanged KMS-5 (defined as KMS-5-Eu) was fully characterized to explore the capture mechanism. SEM image shows that the flaky crystalline form did not change (Figure S8). EDS mapping confirms that KMS-5-Eu is composed of Eu, In, Sn, and S elements (Figure 3a). The homogeneous distribution of Eu (red color) is observed on the KMS-5-Eu sample and almost no K element is found, which indicates that K^+ is completely exchanged out by Eu^{3+} . The final formula of KMS-5-Eu was determined as $[\text{Eu}(\text{H}_2\text{O})_9]_{0.3}\text{InSn}_2\text{S}_6$ (Figure S9). The ion-exchange process is also confirmed by PXRD patterns (Figure 3b). An obvious shift of the (003) and (006)

Bragg peaks to lower diffraction angles in KMS-5-Eu is found as compared with the pristine material. The corresponding interlayer distance is increased from 8.61 to 10.95 Å. Considering the size of Eu^{3+} (109 pm) is smaller than K^+ (152 pm),¹⁸ the Eu species entering in the gallery would not be the bare Eu^{3+} . We deduce that Eu^{3+} might bind with water in the form of hydrated Eu, normally as $\text{Eu}(\text{H}_2\text{O})_{8-9}$,¹⁹ which well coincides with the result of EDS.

Furthermore, XPS spectra of KMS-5-Eu confirm the appearance of Eu peaks and disappearance of K occur as compared with the original material (Figures 3c). The characteristic peaks of Eu 3d and K 2p are shown in Figure S10. The narrow scan spectrum of Eu 3d exhibits a doublet characteristic. Generally, spectra of lanthanides with an incompletely occupied f-subshell exhibit splitting into two separate signals.²⁰ The satellite peaks are 10 eV below the Eu 3d_{5/2} and Eu 3d_{3/2} parent peaks in KMS-5-Eu sample. The binding energy of Eu 3d_{5/2} peaks are 1138.8/1128.7 eV in KMS-5-Eu. These two values are slightly higher than those of $\text{Eu}(\text{NO}_3)_3$ (1136.4/1126.0 eV),²⁰ which might be due to the substitution of nitrate by water and the electrostatic interaction between the negative metal sulfide layers and the $\text{Eu}(\text{H}_2\text{O})_{9}^{3+}$ ions. We did not observe any changes of oxidation states during the ion-exchange process. The optical absorption edge of KMS-5 is 2.27 eV and it blue-shifts slightly to 2.34 eV in the KMS-5-Eu sample (Figure S11).

The composition of HLLW is very complicated and contains a variety of elements including actinides, fission products, and activation products. We tested the separation performance of ^{241}Am and ^{152}Eu in the presence of large excess of Cs^+ , Sr^{2+} , and Ni^{2+} (molar ratio: ~ 2000) at pH 2. As shown in Figure 4a, the

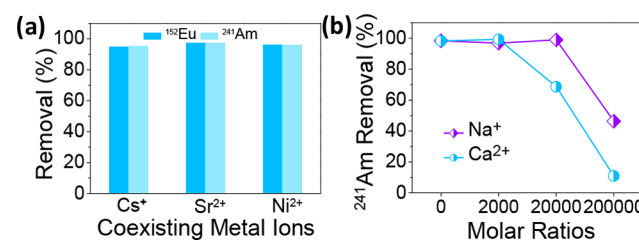


Figure 4. (a) Effect of respective Cs^+ , Sr^{2+} , and Ni^{2+} (molar ratio: ~ 2000) copresent on the removal of ^{241}Am and ^{152}Eu at pH 2. (b) Removal of ^{241}Am at pH 2 as a function of different molar ratios of Na^+ and Ca^{2+} to ^{241}Am (0–200 000).

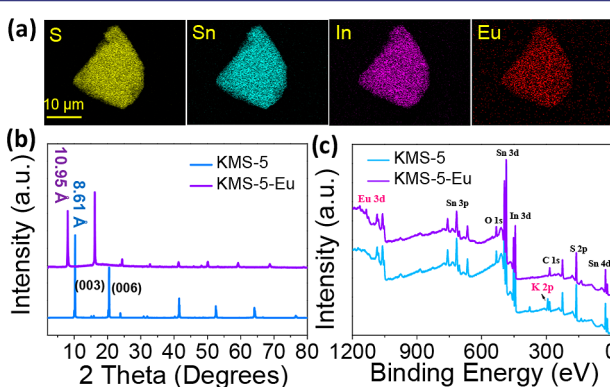


Figure 3. (a) SEM-EDS mapping of Eu^{3+} -exchanged KMS-5. (b) PXRD patterns and (c) XPS spectra of KMS-5 before and after ion exchange.

KMS-5 exhibits an exceptional removal toward ^{241}Am and ^{152}Eu in all the tested cases. The removal rates are in the range of 94.8–98.0% with a high K_d value above 1.8×10^4 mL/g. In addition, KMS-5 can remove nearly 97.7% of ^{241}Am from a simulated nuclear waste stream (Table S3). Such excellent results imply that KMS-5 is a promising ion exchanger to simultaneously separate trivalent minor actinides and lanthanides from HLLW. Furthermore, in the contaminated environmental wastewater, large amounts of Na^+ and Ca^{2+} usually exist, which may be strong competitors for ion exchange of actinide. Thus, the effect of Na^+ and Ca^{2+} on the removal of ^{241}Am by KMS-5 was also investigated (Figure 4b). Na^+ shows weaker influence on the removal of ^{241}Am than Ca^{2+} . In the presence of tremendous excess of Na^+ (20000 times), the removal of ^{241}Am reaches as high as 98.9% (9.4×10^4 mL/g). Even at the molar ratio ($\text{Na}^+/\text{Am}^{241}$) of 200 000, the uptake of ^{241}Am still has 46.3%. Due to higher charge density, Ca^{2+} has a relatively

greater impact on the removal of ^{241}Am , but the K_d is still as high as $2.2 \times 10^3 \text{ mL/g}$ at the molar ratio ($\text{Ca}^{2+}:\text{Am}^{2+}$) of 20 000, corresponding to 68.6% removal. Such high removal rate shows that KMS-5 has good prospect for removing trace amount of ^{241}Am from real radiotoxic water even in the presence of large amounts of Na^+ and Ca^{2+} .

To evaluate the reusability of KMS-5, a high concentration solution of KCl was used to desorb the ^{241}Am -loaded KMS-5. It is found that ^{241}Am can be easily eluted by 1 M KCl. The desorption percentage reaches as high as 97.5% as measured by LSC. The desorption process was also confirmed by PXRD and EDS with Eu^{3+} as a surrogate. As shown in Figures S12 and S13, the desorbed sample has the structure and composition of KMS-5. This result indicates KMS-5 is a reversible ion-exchanger for capturing minor actinides.

In conclusion, KMS-5 exhibits fast kinetics, high capacity, large distribution coefficient, excellent removal, and reversible exchange toward ^{241}Am . This work clearly implies that KMS-5 is a promising ion-exchanger for removing trivalent minor actinides from highly acidic solutions and reveals new directions in the design of novel acid-stable layered metal sulfides sorbents for HLLW treatment and environmental remediation.

■ ASSOCIATED CONTENT

Supporting Information

The Supporting Information is available free of charge on the ACS Publications website at DOI: [10.1021/jacs.7b10464](https://doi.org/10.1021/jacs.7b10464).

Experimental details, spectroscopic and crystallographic data ([PDF](#))
.cif file for KInSn_2S_6 ([CIF](#))

■ AUTHOR INFORMATION

Corresponding Authors

*xuchao@tsinghua.edu.cn

*m-kanatzidis@northwestern.edu

ORCID

Chengliang Xiao: 0000-0001-5081-2398

Chao Xu: 0000-0001-5539-4754

Mercouri G. Kanatzidis: 0000-0003-2037-4168

Notes

The authors declare no competing financial interest.

■ ACKNOWLEDGMENTS

This work was supported by the U.S. National Science Foundation (DMR-1708254) and grants from the National Natural Science Foundation of China (11605118, 21571114, U1732112), the Natural Science Foundation of Jiangsu Province (BK20150313), China Scholarship Council.

■ REFERENCES

- (1) (a) Zhu, L.; Sheng, D. P.; Xu, C.; Dai, X.; Silver, M. A.; Li, J.; Li, P.; Wang, Y. X.; Wang, Y. L.; Chen, L. H.; Xiao, C. L.; Chen, J.; Zhou, R. H.; Zhang, C.; Farha, O. K.; Chai, Z. F.; Albrecht-Schmitt, T. E.; Wang, S. A. *J. Am. Chem. Soc.* **2017**, *139*, 14873–14876. (b) Sheng, D. P.; Zhu, L.; Xu, C.; Xiao, C. L.; Wang, Y. L.; Wang, Y. X.; Chen, L. H.; Diwu, J.; Chen, J.; Chai, Z. F.; Albrecht-Schmitt, T. E.; Wang, S. A. *Environ. Sci. Technol.* **2017**, *51*, 3471–3479.
- (2) Dares, C. J.; Lapidés, A. M.; Mincher, B. J.; Meyer, T. J. *Science* **2015**, *350*, 652–655.
- (3) Salvatores, M.; Palmiotti, G. *Prog. Part. Nucl. Phys.* **2011**, *66*, 144–166.

- (4) (a) Mathur, J. N.; Murali, M. S.; Nash, K. L. *Solvent Extr. Ion Exch.* **2001**, *19*, 357–390. (b) Modolo, G.; Wilden, A.; Geist, A.; Magnusson, D.; Malmbeck, R. *Radiochim. Acta* **2012**, *100*, 715–725. (c) Panak, P. J.; Geist, A. *Chem. Rev.* **2013**, *113*, 1199–1236.

- (5) Berrueta, L. A.; Gallo, B.; Vicente, F. *Chromatographia* **1995**, *40*, 474–483.

- (6) Horwitz, E. P.; McAlister, D. R.; Dietz, M. L. *Sep. Sci. Technol.* **2006**, *41*, 2163–2182.

- (7) Shehee, T. C.; Elvington, M. C.; Rudisill, T. S.; Hobbs, D. T. *Solvent Extr. Ion Exch.* **2012**, *30*, 669–682.

- (8) Silbernagel, R.; Shehee, T. C.; Martin, C. H.; Hobbs, D. T.; Clearfield, A. *Chem. Mater.* **2016**, *28*, 2254–2259.

- (9) Wang, X.; Yang, S.; Shi, W.; Li, J.; Hayat, T.; Wang, X. *Environ. Sci. Technol.* **2015**, *49*, 11721–11728.

- (10) (a) Florek, J.; Giret, S.; Juere, E.; Lariviere, D.; Kleitz, F. *Dalton Trans.* **2016**, *45*, 14832–54. (b) Zhang, W.; He, X.; Ye, G.; Yi, R.; Chen, J. *Environ. Sci. Technol.* **2014**, *48*, 6874–6881.

- (11) Romanchuk, A. Y.; Slesarev, A. S.; Kalmykov, S. N.; Kosynkin, D. V.; Tour, J. M. *Phys. Chem. Chem. Phys.* **2013**, *15*, 2321–2327.

- (12) Demir, S.; Brune, N. K.; Van Humbeck, J. F.; Mason, J. A.; Plakhova, T. V.; Wang, S.; Tian, G.; Minasian, S. G.; Tyliszczak, T.; Yaita, T.; Kobayashi, T.; Kalmykov, S. N.; Shiwaku, H.; Shuh, D. K.; Long, J. R. *ACS Cent. Sci.* **2016**, *2*, 253–65.

- (13) (a) Manos, M. J.; Ding, N.; Kanatzidis, M. G. *Proc. Natl. Acad. Sci. U. S. A.* **2008**, *105*, 3696–3699. (b) Manos, M. J.; Kanatzidis, M. G. *J. Am. Chem. Soc.* **2009**, *131*, 6599–6607. (c) Manos, M. J.; Kanatzidis, M. G. *Chem. - Eur. J.* **2009**, *15*, 4779–4784. (d) Manos, M. J.; Petkov, V. G.; Kanatzidis, M. G. *Adv. Funct. Mater.* **2009**, *19*, 1087–1092. (e) Manos, M. J.; Kanatzidis, M. G. *J. Am. Chem. Soc.* **2012**, *134*, 16441–16446. (f) Mertz, J. L.; Fard, Z. H.; Malliakas, C. D.; Manos, M. J.; Kanatzidis, M. G. *Chem. Mater.* **2013**, *25*, 2116–2127. (g) Feng, M. L.; Sarma, D.; Qi, X. H.; Du, K. Z.; Huang, X. Y.; Kanatzidis, M. G. *J. Am. Chem. Soc.* **2016**, *138*, 12578–12585. (h) Manos, M. J.; Kanatzidis, M. G. *Chem. Sci.* **2016**, *7*, 4804–4824. (i) Sarma, D.; Malliakas, C. D.; Subrahmanyam, K. S.; Islam, S. M.; Kanatzidis, M. G. *Chem. Sci.* **2016**, *7*, 1121–1132. (j) Ma, S. L.; Huang, L.; Ma, L. J.; Shim, Y.; Islam, S. M.; Wang, P. L.; Zhao, L.-D.; Wang, S. C.; Sun, G. B.; Yang, X. J.; Kanatzidis, M. G. *J. Am. Chem. Soc.* **2015**, *137*, 3670–3677.

- (14) Richards, J. M.; Sudowe, R. *Anal. Chem.* **2016**, *88*, 4605–4608.

- (15) Banerjee, C.; Dudwadkar, N.; Tripathi, S. C.; Gandhi, P. M.; Grover, V.; Kaushik, C. P.; Tyagi, A. K. *J. Hazard. Mater.* **2014**, *280*, 63.

- (16) (a) Tan, X.; Fang, M.; Li, J.; Lu, Y.; Wang, X. *J. Hazard. Mater.* **2009**, *168*, 458–465. (b) Shao, D.; Fan, Q.; Li, J.; Niu, Z.; Wu, W.; Chen, Y.; Wang, X. *Microporous Mesoporous Mater.* **2009**, *123*, 1–9.

- (c) Sun, Y.; Li, J.; Wang, X. *Geochim. Cosmochim. Acta* **2014**, *140*, 621–643. (d) Gad, H. M. H.; Awwad, N. S. *Sep. Sci. Technol.* **2007**, *42*, 3657–3680.

- (17) (a) Li, C.; Huang, Y.; Lin, Z. *J. Mater. Chem. A* **2014**, *2*, 14979–14985. (b) Sun, Y.; Wang, Q.; Chen, C.; Tan, X.; Wang, X. *Environ. Sci. Technol.* **2012**, *46*, 6020–6027. (c) Qi, X. H.; Du, K. Z.; Feng, M. L.; Gao, Y. J.; Huang, X. Y.; Kanatzidis, M. G. *J. Am. Chem. Soc.* **2017**, *139*, 4314–4317.

- (18) Shannon, R. D. *Acta Crystallogr., Sect. A: Cryst. Phys., Diffr., Theor. Gen. Crystallogr.* **1976**, *32*, 751–767.

- (19) Persson, I. *Pure Appl. Chem.* **2010**, *82*, 1901–1917.

- (20) Mercier, F.; Alliot, C.; Bion, L.; Thromat, N.; Toulhoat, P. J. *Electron Spectrosc. Relat. Phenom.* **2006**, *150*, 21–26.